Luminescence Switches of a Persistent Room-Temperature Phosphorescent Pure Organic Molecules in Response to External Stimuli

Pengchong Xue,*[a] Jiabao Sun,[a] Peng Chen,[b] Panpan Wang,[a] Boqi Yao,[a] Peng Gong,[a] Zhenqi Zhang[a] and Ran Lu*[a]

[a] State Key Laboratory of Supramolecular Structure and Materials, College of Chemistry, Jilin University, 2699 Qianjin Street, Changchun, P.R. China

[b] Key Laboratory of Functional Inorganic Material Chemistry (MOE), Chemistry and Materials Science, Heilongjiang University, No. 74, Xuefu Road, Nangang District, Harbin, P. R. China

E-mail: xuepengchong@jlu.edu.cn; luran@mail.jlu.edu.cn

EXPERIMENTAL SECTION

Instruments and experimental methods: Infrared spectra were measured using a Nicolet-360 FT-IR spectrometer by incorporating the samples in KBr disks. The UV-vis spectra were determined on a Mapada UV-1800pc spectrophotometer. C, H, and N elemental analyses were performed on a Perkin-Elmer 240C elemental analyzer. Photoluminescence measurements were taken on a Shimadzu RF-5301 Luminescence Spectrometer. The absolute fluorescence quantum yields were measured on an Edinburgh FLS920 steady state spectrometer using an integrating sphere. Luminescent decay experiments were measured on an Edinburgh FLS920 spectrometer. EPLED-360 picosecond flash lamp with 898ps pulse duration and μF920 microsecond flash lamp (pulse width < 2 μs) were used to measure time-resolved fluorescent and phosphorescent spectra, respectively. ^{1}H and ^{13}C NMR spectra were recorded on Mercury plus 400 MHz. The fluorescence quantum yields of **CBA** in different solvents were measured by comparing to standards (quinine sulfate in 1 M H_2SO_4 aqueous solution, $\Phi_F = 0.65$). The XRD patterns were obtained on an Empyrean X-ray diffraction instrument equipped with graphite-mono-chromatized CuK_α radiation ($\lambda = 1.5418$ Å), by employing a scanning rate of 0.026° s^{-1} in the 2θ range from 5 to 30°. Geometrical optimization for **CBA** was performed by density functional theory (DFT) calculations at B3LYP/6-31G (d, p) level with the Gaussian 09W program package. Electronic transition data obtained by the TD/DFT-B3LYP/6-31G(d,p) calculation based on the configuration at ground state.

Carbazole (≥95%) and 4-bromobenzaldehyde (99%) were purchased from Aldrich, other chemicals purchased from Sinopharm Chemical Reagent Co.,Ltd.

Single crystal of **CBA** was obtained by slowing solvent evaporation in *n*-hexane and selected for X-ray diffraction analysis on in a Rigaku RAXIS-RAPID diffractometer using graphite-monochromated Mo-K_α radiation (λ = 0.71073 Å). The crystal was kept at room temperature during data collection. The structures were solved by the direct methods and refined on F2 by full-matrix least-square using the SHELXTL-97 program. The C, N, O and H atoms were easily placed from the subsequent Fourier-difference maps and refined anisotropically. CCDC 1037574 contains the supplementary crystallographic data for this paper.

Synthesis of BVDA

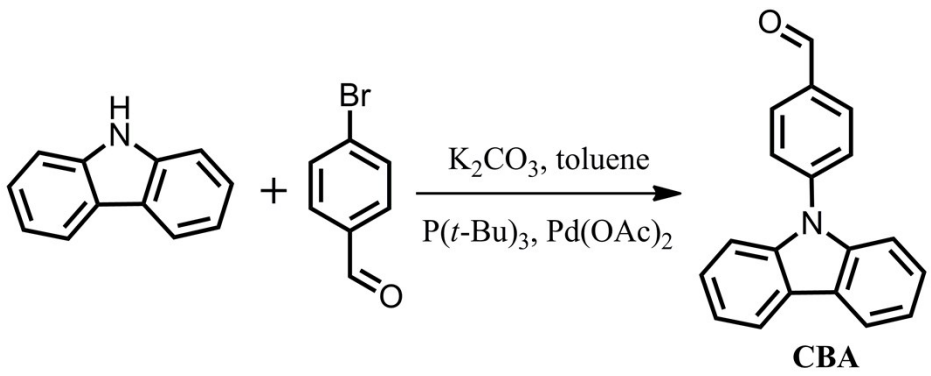

Scheme S1 Synthesis route of **CBA**.

4-(9H-carbazol-9-yl)benzaldehyde (**CBA**)

The mixture of carbazole (2.0 g, 12 mmol), 4-bromobenzaldehyde (2.5 g, 13.5 mmol), K_2CO_3 (4.15 g, 30 mmol), palladium acetate (0.2 g, 1.0 mmol), tri-tert-butylphosphine (0.3 ml, 1.2 mmol) in 20 ml of anhydrous toluene was refluxed 24 h under nitrogen atmosphere. After the solvent was moved, the residue was purified by column chromatography (petroleum ether/CH_2Cl_2, V/V = 1: 1) to afford 2.3 white solid (71% in yield). Element analysis (%): calculated for $C_{19}H_{13}NO$: C, 84.11; H, 4.83; N, 5.16; found: C, 84.16; H, 4.78; N, 5.12. ^{1}H NMR (400 MHz, $CDCl_3$) δ 10.11 (s, 1H), 8.14 (t, J = 7.4 Hz, 4H), 7.79 (d, J = 8.2 Hz, 2H), 7.50 (d, J = 8.2 Hz, 2H), 7.43 (t, J = 7.6 Hz, 2H), 7.33 (t, J = 7.4 Hz, 2H). ^{13}C NMR (101 MHz, $CDCl_3$) δ 190.99, 143.43, 140.09, 134.68, 131.41, 126.87, 126.31, 123.99, 120.84, 120.53, 109.78.

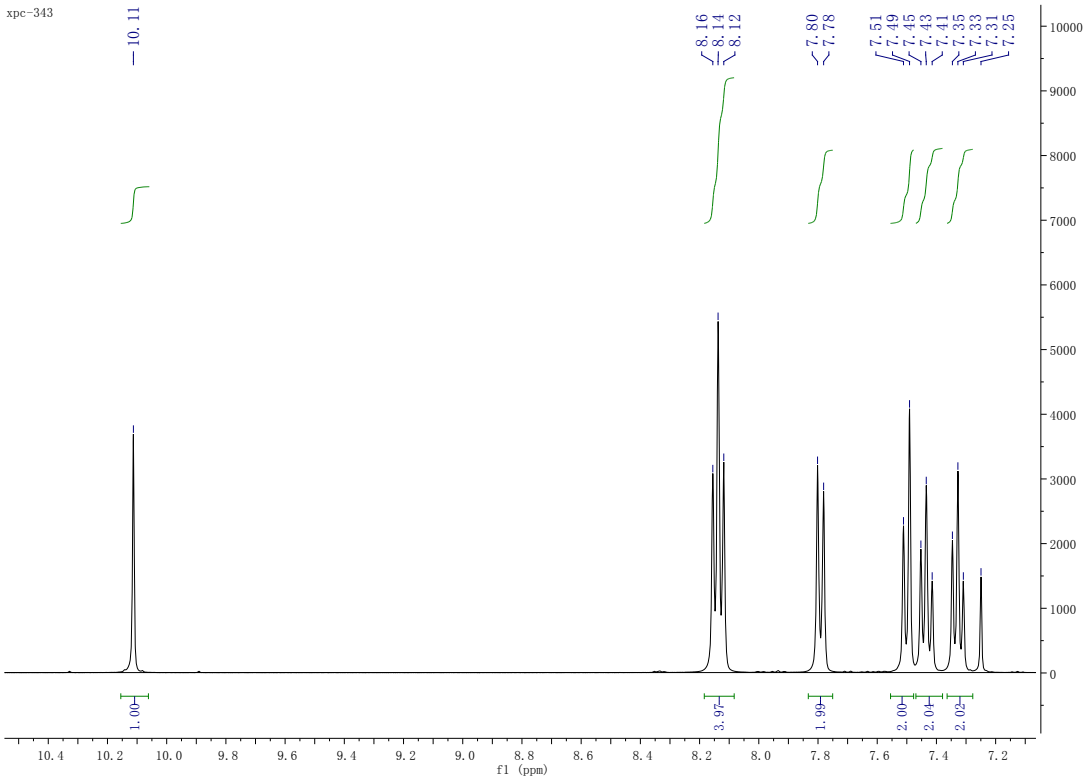

Fig. S1 ^{1}H NMR of **CBA** in $CDCl_3$.

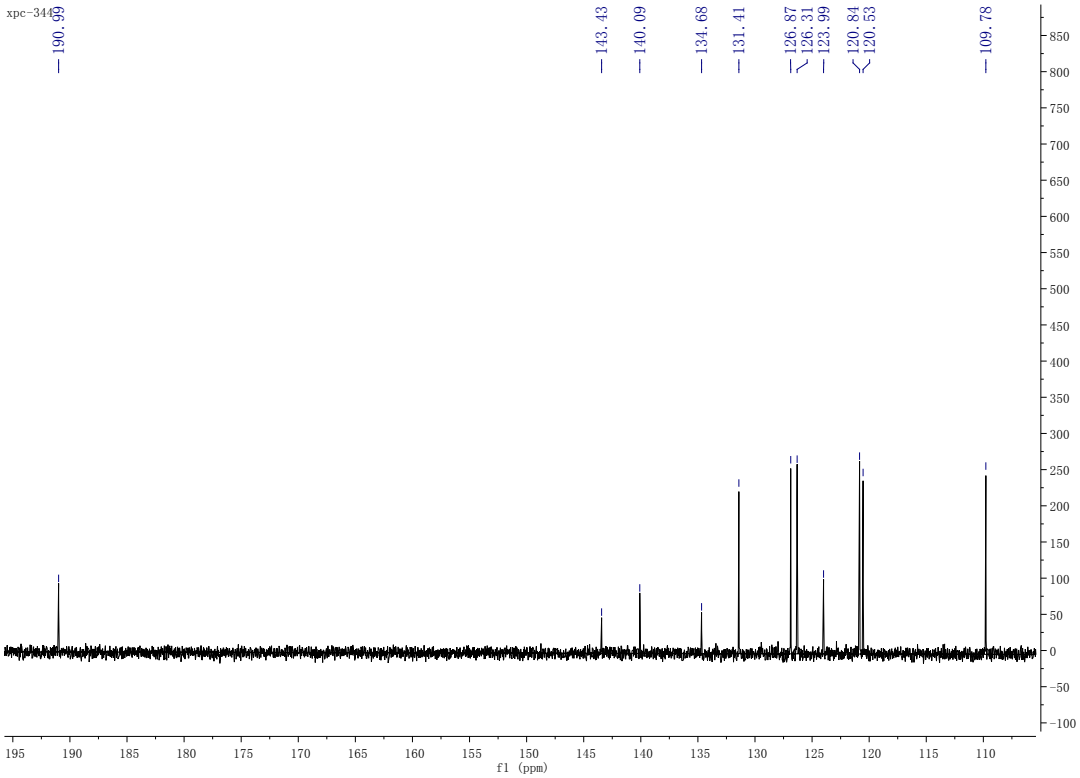

Fig. S2 ^{13}C NMR of **CBA** in $CDCl_3$.

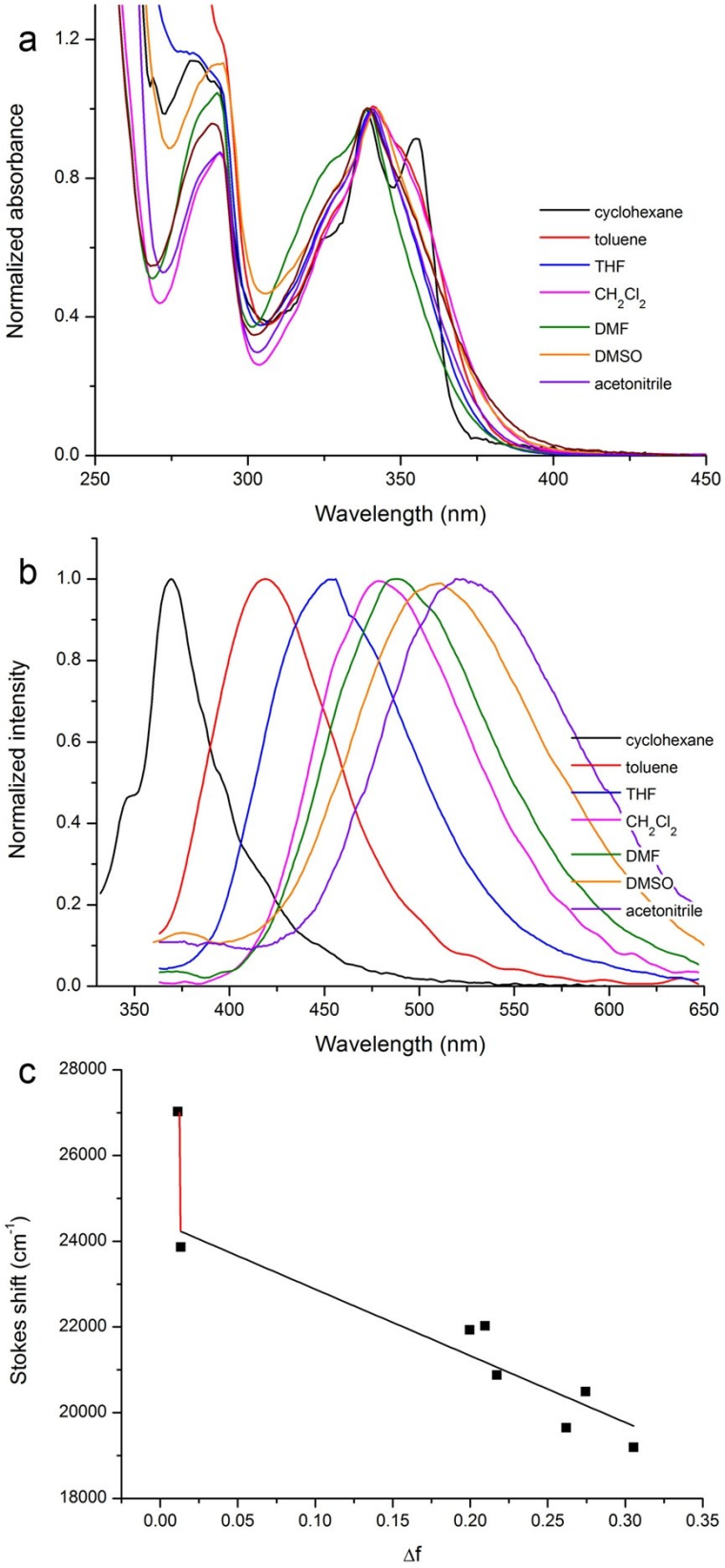

Fig. S3 Absorption (a) and fluorescence (b) spectra of **CBA** in different solvents and the Lippert-Mataga plot (c).

Table S1 Absorption and fluorescence data of **CBA** in different solvents.

solvents	λ_{abs} (nm)	λ_{em} (nm)	Φ
Cyclohexane	339	370	0.048
Toluene	341	419	0.058
THF	340	454	0.047
CH_2Cl_2	341.5	478	0.28
DMF	339	487	0.12
DMSO	342	508	0.09
Acetonitrile	341	522	0.017

Table S2. Computed vertical excitation spectra of **CBA** in cyclohexane based on the optimal structure at ground state.

Transition	Transition assignment	Transition type	E (eV)	λ_{abs} (nm)	Oscillator strength
$S_0 \rightarrow S_1$	HOMO→LUMO (100%)	π-π*	3.1896	388.71	0.2631
$S_0 \rightarrow T_3$	HOMO-6→LUMO+5 (3.1%)	π-π*	3.1626	392.04	0.0000
	HOMO-3→LUMO (18.4%)	n-π*			
	HOMO-2→LUMO+1 (3.2%)	n-π*			
	HOMO-2→LUMO+4 (2.4%)	n-π*			
	HOMO-1→LUMO (6.8%)	π-π*			
	HOMO-1→LUMO+1 (55.8%)	π-π*			
	HOMO→LUMO+3 (10.2%)	π-π*			
$S_0 \rightarrow T_2$	**HOMO-3→LUMO (71.2%)**	n-π*	3.1531	393.21	0.0000
	HOMO-3→LUMO+4 (4.1%)	n-π*			
	HOMO-2→LUMO (7.6%)	n-π*			
	HOMO-1→LUMO (2.3%)	π-π*			
	HOMO-1→LUMO+1 (12.5%)	π-π*			
	HOMO→LUMO+3 (2.3%)	π-π*			
$S_0 \rightarrow T_1$	HOMO-4→LUMO (13.8%)	π-π*	2.7452	451.65	0.0000
	HOMO→LUMO (86.2%)	π-π*			

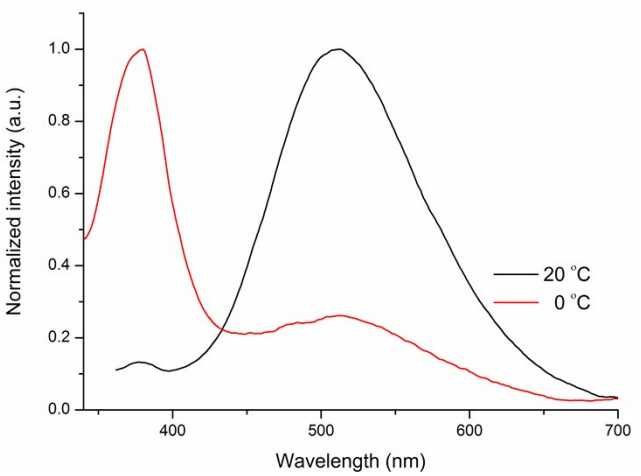

Fig. S4 Fluorescence spectra of **CBA** in DMSO (10^{-5} M) at 20 ºC and 0 ºC.

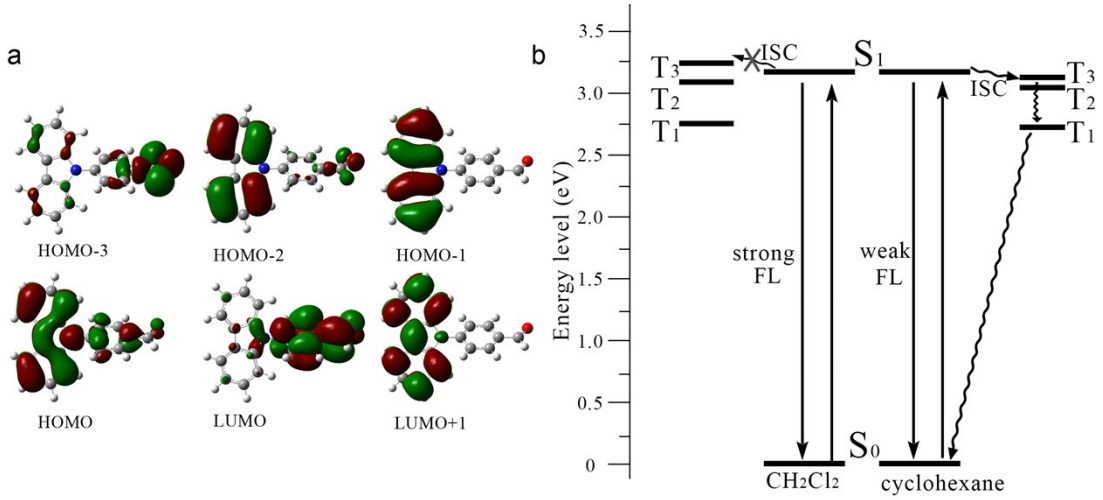

Fig. S5 (a) Frontier molecular orbitals of **CBA**, and (b) Energy levels of the singlet and triplet states in cyclohexane and CH_2Cl_2, which obtained by quantum chemical calculation.

Table S3. Computed vertical excitation spectra of **CBA** in CH_2Cl_2 based on the optimal structure at ground state.

Transition	Transition assignment	Transition type	E (eV)	λ_{abs} (nm)	Oscillator strength
$S_0 \rightarrow S_1$	HOMO→LUMO (100%)	π-π*	3.1939	388.19	0.2646
$S_0 \rightarrow T_3$	**HOMO-3→LUMO (89.6%)**	n-π*	3.2013	387.29	0.0000
	HOMO-3→LUMO+4 (3.8%)	n-π*			
	HOMO-3→LUMO+6 (2.7%)	n-π*			
	HOMO-2→LUMO (4.0%)	n-π*			
$S_0 \rightarrow T_2$	HOMO-6→LUMO+5 (3.9%)	π-π*	3.1626	392.04	0.0000
	HOMO-2→LUMO+4 (2.2%)	n-π*			
	HOMO-2→LUMO+1 (4.2%)	n-π*			
	HOMO-1→LUMO (8.8%)	π-π*			
	HOMO-1→LUMO+1 (68.3%)	π-π*			
	HOMO→LUMO+3 (12.7%)	π-π*			
$S_0 \rightarrow T_1$	HOMO-4→LUMO (13.8%)	π-π*	2.7467	451.39	0.0000
	HOMO→LUMO (86.2%)	π-π*			

Table S4. Energy levels of orbital in cyclohexane and CH_2Cl_2.

orbital	cyclohexane[a] eV	CH_2Cl_2 eV
LUMO+5	1.02272	0.99661
LUMO+4	0.38488	0.3672
LUMO+3	0.01686	-0.01084
LUMO+2	-0.6158	-0.57074
LUMO+1	-0.88935	-0.91676
LUMO	**-1.91145**	**-1.92849**
HOMO	**-5.60339**	**-5.62188**
HOMO-1	-5.95573	-5.98745
HOMO-2	**-6.98666**	**-7.01576**
HOMO-3	**-7.09251**	**-7.15366**
HOMO-4	-7.33911	-7.33437
HOMO-5	-7.46234	-7.42135
HOMO-6	-7.75552	-7.78448

[a] HOMO-2 and HOMO-3 are n^2 configuration; HOMO and LUMO are π orbitals.

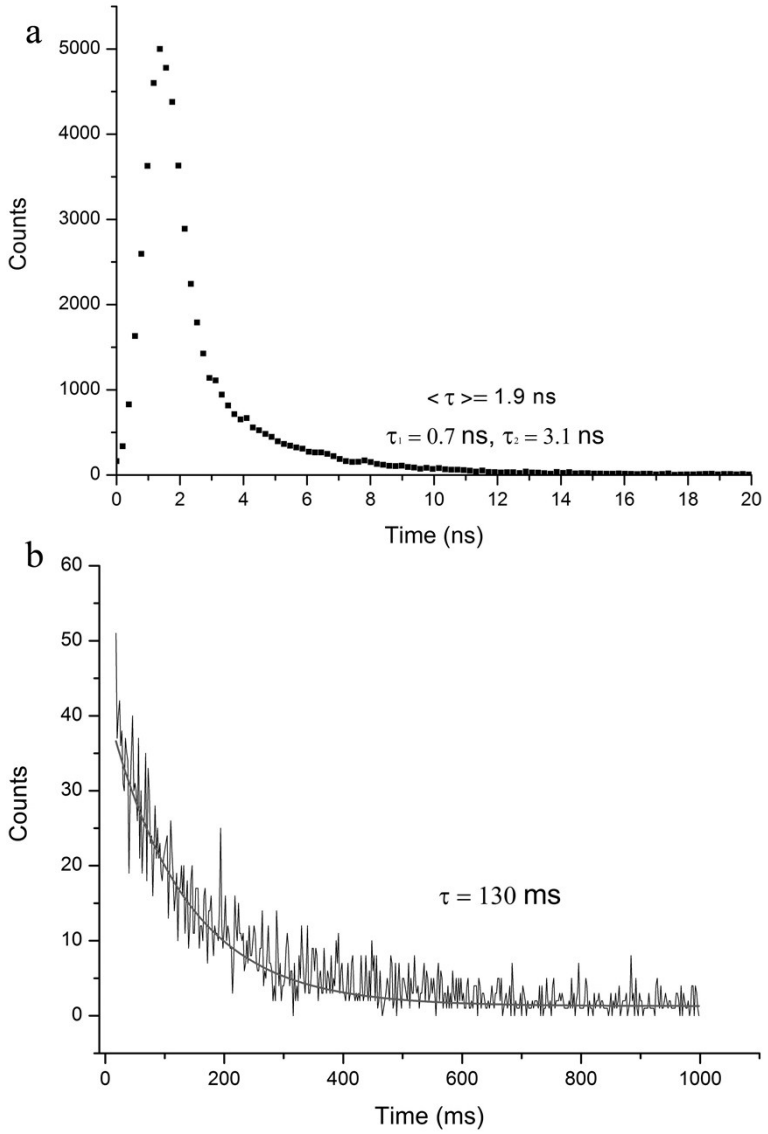

Fig. S6 Decay curves of **CBA** with different excitation sources. λ_{ex}= 360 nm, λ_{em}= 450 nm.

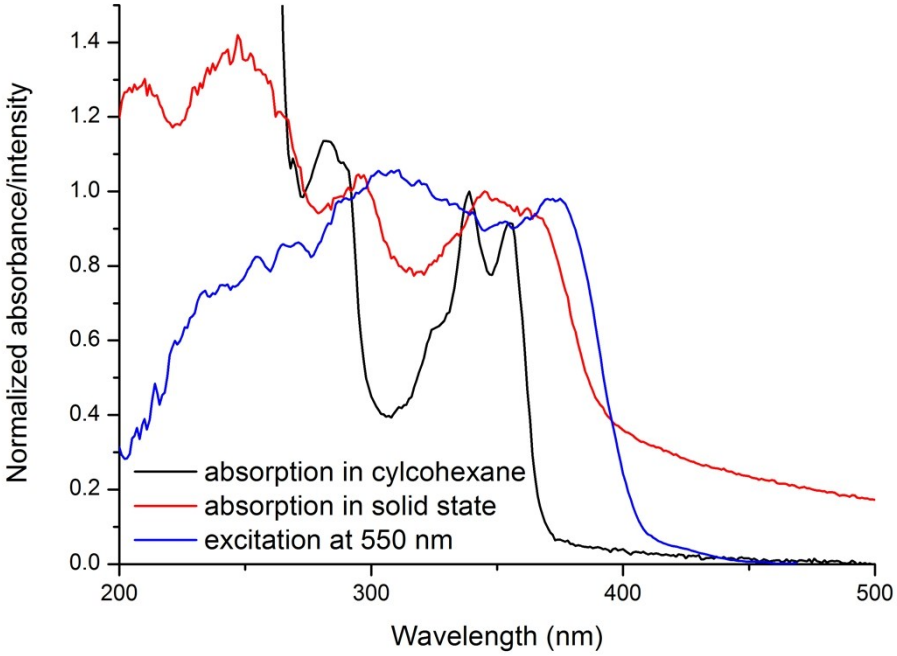

Fig. S7 Absorption and excitation spectra of **CBA** in cyclohexane and solid state. λ_{em} = 550 nm.

Table S5. Computed vertical excitation spectra of **CBA** based on the molecular conformation in crystal at ground state.

Transition		Transition type	E (eV)	λ_{abs} (nm)	Oscillator strength
$S_0 \rightarrow S_1$	HOMO→LUMO (100%)		3.4217	362.35	0.2041
$S_0 \rightarrow T_3$	HOMO-3→LUMO (48.0%)	n-π*	3.3801	366.81	0.0000
	HOMO-3→LUMO+4 (2.1%)	n-π*			
	HOMO-2→LUMO (47.7%)	n-π*			
	HOMO-2→LUMO+4 (2.1%)	n-π*			
$S_0 \rightarrow T_2$	HOMO-6→LUMO+5 (3.7%)	π-π*	3.2705	379.10	0.0000
	HOMO-2→LUMO+1 (2.6%)	n-π*			
	HOMO-1→LUMO (4.6%)	π-π*			
	HOMO-1→LUMO+1 (76.3%)	π-π*			
	HOMO→LUMO+3 (12.7%)	π-π*			
$S_0 \rightarrow T_1$	HOMO-5→LUMO+2 (2.1%)	π-π*	2.9592	418.98	0.0000
	HOMO-4→LUMO (11.3%)	π-π*			
	HOMO→LUMO (86.6%)	π-π*			

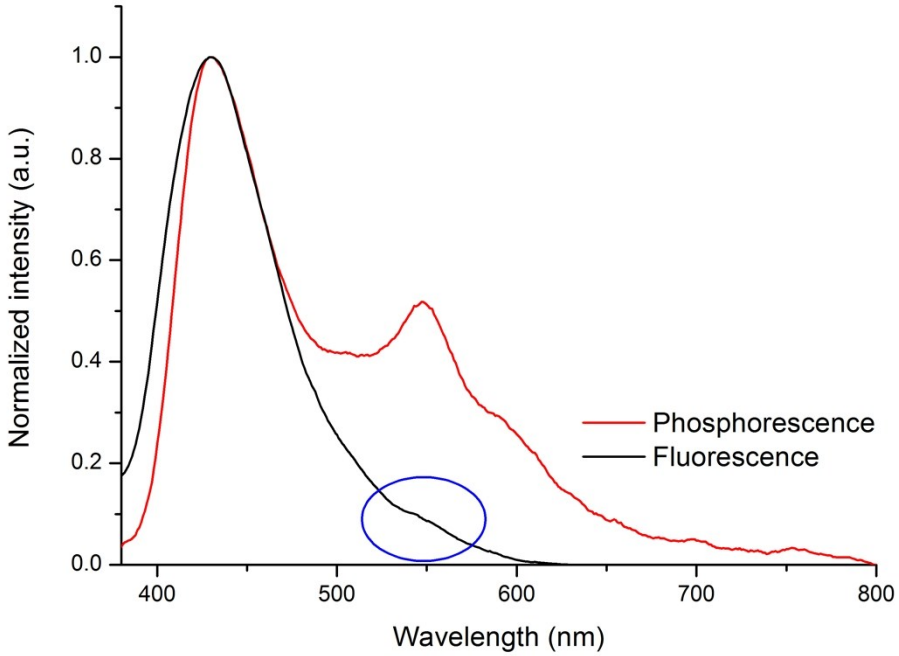

Fig. S8 Photoluminescence (red) and phosphorescence spectra of ground powder under excitation at 360 nm. Blue circle shows weak emission bands from phosphorescence.

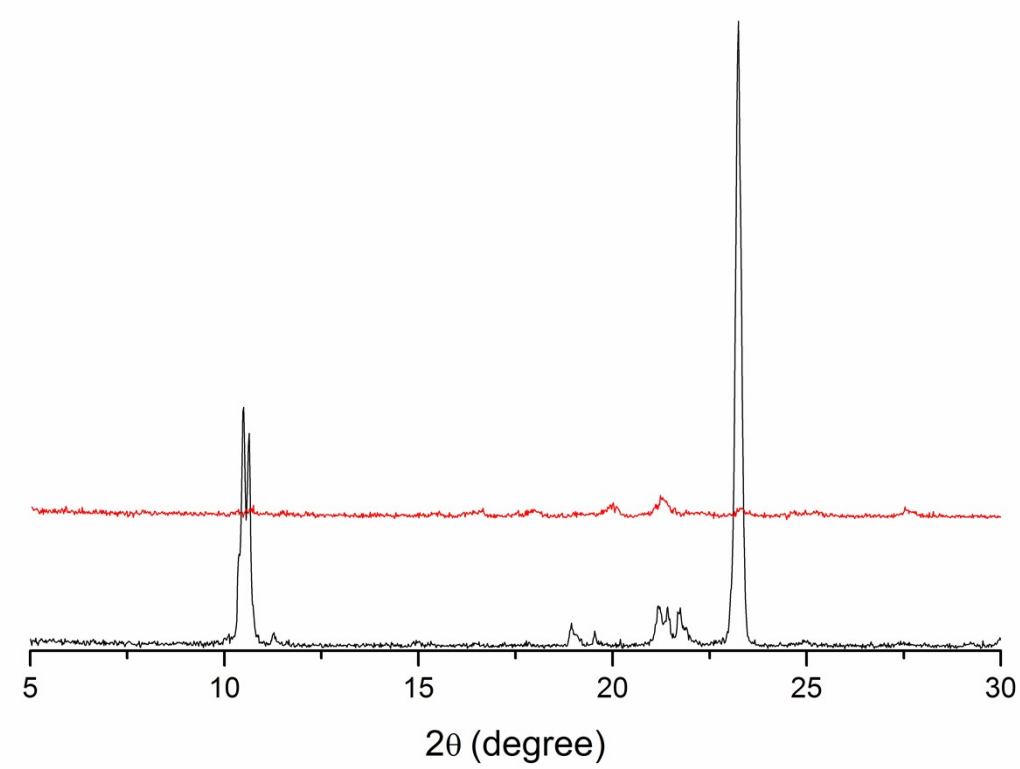

Fig. S9 XRD patterns of **CBA** in crystal (black) and ground powders (red) after aging 10 min.

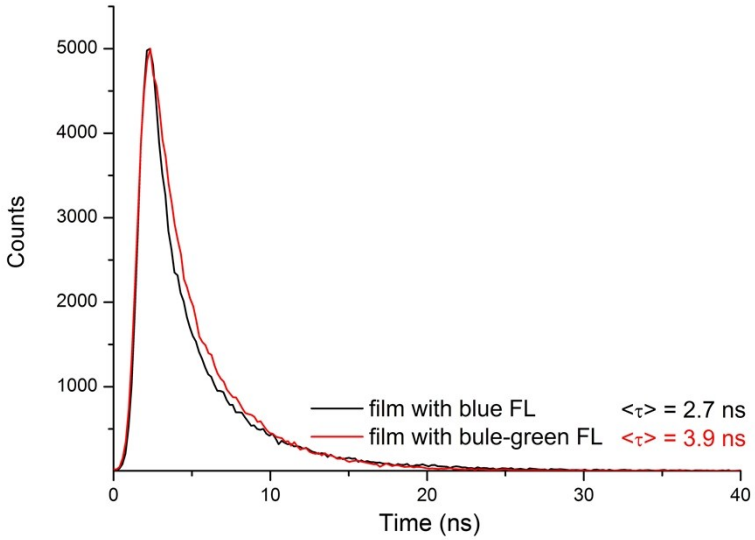

Fig. S10 Fluorescence decay curves of **CBA** after grinding and further grinding on the surface of filter. λ_{ex} = 360 nm, λ_{ex} = 450 nm.